Inorganic Chemistry

Article

pubs.acs.org/IC

Solution Dynamics of Redox Noninnocent Nitrosoarene Ligands: Mapping the Electronic Criteria for the Formation of Persistent Metal-Coordinated Nitroxide Radicals

Brandon R. Barnett,[†] Liezel A. Labios,[†] Curtis E. Moore,[†] Jason England,[‡] Arnold L. Rheingold,[†] Karl Wieghardt,[‡] and Joshua S. Figueroa*[,†]

[†]Department of Chemistry and Biochemistry, University of California San Diego, 9500 Gilman Drive, MC 0358, La Jolla, California 92093-0358, United States

[‡]Max Planck Institute for Chemical Energy Conversion, Stiftstrasse 34−36, D-45470 Mülheim an der Ruhr, Germany

Supporting Information

ABSTRACT: The redox-noninnocence of metal-coordinated *C*-organo nitrosoarenes has been established on the basis of solid-state characterization techniques, but the solution-phase properties of this class of metal-coordinated radicals have been relatively underexplored. In this report, the solution-phase properties and dynamics of the bis-nitrosobenzene diradical complex *trans*-Pd(κ^1-*N*-PhNO)$_2$(CNAr^{Dipp2})$_2$ are presented. This complex, which is best described as containing singly reduced phenylnitroxide radical ligands, is shown to undergo facile nitrosobenzene dissociation in solution to form the metalloxaziridine Pd(η^2-*N*,*O*-PhNO)(CNAr^{Dipp2})$_2$ and thus is not a persistent species in solution. An equilibrium between *trans*-Pd(κ^1-*N*-PhNO)$_2$(CNAr^{Dipp2})$_2$, Pd(η^2-*N*,*O*-PhNO)(CNAr^{Dipp2})$_2$, and free nitrosobenzene is established in solution, with the metalloxaziridine being predominantly favored. Efforts to perturb this equilibrium by the addition of excess nitrosobenzene reveal that the formation of *trans*-Pd(κ^1-*N*-PhNO)$_2$(CNAr^{Dipp2})$_2$ is in competition with insertion-type chemistry of Pd(η^2-*N*,*O*-PhNO)(CNAr^{Dipp2})$_2$ and is therefore not a viable strategy for the production of a kinetically persistent bis-nitroxide radical complex. Electronic modification of the nitrosoarene framework was explored as a means to generate a persistent *trans*-Pd(κ^1-*N*-ArNO)$_2$(CNAr^{Dipp2})$_2$ complex. While most substitution schemes failed to significantly perturb the kinetic lability of the nitrosoarene ligands in the corresponding *trans*-Pd(κ^1-*N*-ArNO)$_2$(CNAr^{Dipp2})$_2$ complexes, utilization of *para*-formyl or *para*-cyano nitrosobenzene produced bis-nitroxide diradical complexes that display kinetic persistence in solution. The origin of this persistence is rationalized by the ability of *para*-formyl- and *para*-cyano-aryl groups to both attenuate the trans effect of the corresponding nitrosoarene and, more importantly, delocalize spin density away from the aryl-nitroxide NO unit. The results presented here highlight the inherent instability of metal-coordinated nitroxide radicals and suggest a general synthetic strategy for kinetically stabilizing these species in solution.

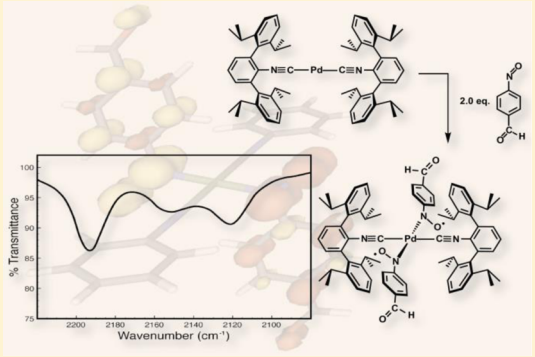

INTRODUCTION

Redox noninnocent ligands offer unique opportunities to modulate the electronic structure and reactivity of transition metal complexes.[1] As opposed to traditional "innocent" ligands, which act as formal spectators in redox transformations, noninnocent ligands can directly participate in the redox activity of coordination complexes due to the presence of ligand frontier orbitals and metal valence *d* orbitals of similar energies. Classical bidentate noninnocent ligand frameworks such as 1,2-dioxolenes[2,3] and 1,2-dithiolenes[4−6] have received extensive study, while the more recent development of larger, polydentate noninnocent systems has led to the discovery of new paradigms in metal-based reactivity and catalysis.[7−15]

Despite the current prevalence of noninnocent ligand systems containing extended π-systems,[16−19] ligand redox participation can be readily observed in simple diatomics such as O_2[20,21] and NO.[22−25] The electronic structures of coordination complexes containing these ligands, along with the related nitroxyl (HNO) molecule,[26] have been extensively investigated, in part due to their relevance and implication in biological systems.[21,25,27−32] Contrastingly, the noninnocent properties of the closely related class of *C*-organonitroso compounds (i.e., O═N−R)[33−35] have been relatively understudied. *C*-Organonitroso compounds are known isoelectronic analogues of singlet dioxygen, and coordination compounds of nitrosoarenes often display structural properties and reactivity reminiscent of those bearing peroxide or superoxide ligands.[36−39] Transition metal compounds bearing nitrosoarenes have also been observed as intermediates in the allylic amination of olefins[40,41] and the metal-mediated deoxygenation of nitroaromatics.[42−44] Most importantly, *C*-organonitroso

Received: June 2, 2015
Published: July 1, 2015

DOI: 10.1021/acs.inorgchem.5b01252
Inorg. Chem. 2015, 54, 7110−7121

compounds have been frequently utilized as spin traps for organic- and transition metal-based radicals,[45,46] with electron paramagnetic resonance (EPR) spectroscopy suggesting that many such spin adducts are best described as nitroxide radicals.[47,48] However, it is critical to note that despite the prevalence of EPR data in spin-trapping experiments, structurally characterized coordination complexes described as containing singly reduced nitroso radical anions (i.e., $[ONR]^{-\cdot}$; isoelectronic to the superoxide anion) are quite few.[38,49−51] This observation is likely tied to the inherent instabilities of many such transition metal-nitroxide radical species, their ill-defined reactivity, and the difficulties associated with assigning formal oxidation states in nitroso-containing complexes.[52]

In our studies of transition metal centers supported by *m*-terphenyl isocyanides,[53−60] we reported that the zerovalent bis-isocyanide $Pd(CNAr^{Dipp2})_2$ (Ar^{Dipp2} = 2,6-(2,6-(*i*-Pr)$_2$-C_6H_3)$_2$$C_6H_3$) reacts with 2 equiv of nitrosobenzene (PhNO) to form the four-coordinate complex *trans*-$Pd(\kappa^1$-*N*-$PhNO)_2(CNAr^{Dipp2})_2$ (**1a**).[49] X-ray crystallography, X-ray absorption spectroscopy (XAS), and computational studies indicated that, in the solid state, complex **1a** possessed a divalent palladium center and two monoanionic nitroxide radicals.[52] In addition, magnetic susceptibility measurements on crystalline samples of **1a** showed that the nitroxide radicals exhibit weak antiferromagnetic coupling mediated by superexchange across the Pd center resulting in a ground-state, open-shell singlet (i.e., singlet diradical) and a triplet excited state that is thermally accessible at ca. 290 K (singlet−triplet gap = 0.4 kcal/mol). Accordingly, **1a** represented a rare example of a well-characterized nitroxide-radical complex formally related to traditional spin-trapping experiments. In addition, treatment of $Pd(CNAr^{Dipp2})_2$ with *ortho*-nitrosotoluene (*o*-TolNO; *o*-MeC_6H_4NO) sterically precluded the formation of a bis-nitroxide radical complex and led to the selective formation of $Pd(\eta^2$-*N*,*O*-TolNO$)(CNAr^{Dipp2})_2$.[52] The latter features a side-on-bound and doubly reduced nitrosoarene ligand (metalloxaziridine), which is best thought of as a doubly deptrotonated *N*-arylhydroxylamine.[61] Importantly, however, *trans*-$Pd(\kappa^1$-*N*-$PhNO)_2(CNAr^{Dipp2})_2$ (**1a**) and $Pd(\eta^2$-*N*,*O*-TolNO$)(CNAr^{Dipp2})_2$ represented the first set of *C*-organo-nitroso analogues to metal-bound κ^1-superoxide and η^2-peroxide on the same coordination platform.

While computational and magnetic studies conclusively elucidated the singly reduced nature of the nitrosobenzene ligands in $Pd(\kappa^1$-*N*-$PhNO)_2(CNAr^{Dipp2})_2$ (**1a**), our preliminary studies of this molecule had reported that it produced well-defined solution NMR spectra characteristic of a diamagnetic molecule.[49] It was realized that this observation conflicted with the solid-state properties of **1a** and indicated more complex behavior for this bis-nitroxide radical species in solution. Furthermore, this discrepancy highlighted the lack of information available for the solution-phase properties and reactivity of coordinated nitroxide ligands in general. Accordingly, here we provide a more complete description of the solution-phase properties and dynamics of the bis-nitroxide radical complex $Pd(\kappa^1$-*N*-$PhNO)_2(CNAr^{Dipp2})_2$ (**1a**) and other nitrosoarene derivatives. Our results demonstrate that, for this system, there is a facile interconversion between κ^1-*N* nitroxide and η^2-*N*,*O* metalloxaziridine forms of coordinated nitrosoarenes. In addition, the relative kinetic stability of κ^1-*N* arylnitroxide radical ligands is sensitive to both the substituent identity and pattern of the aryl group. Most notably, this finding has led to the identification of aryl substituents that promote the formation of kinetically persistent nitroxide radical complexes in solution and has important ramifications for the formation and isolation of metal-coordinated nitroxide radicals generally.

RESULTS AND DISCUSSION

Solution Dynamics of $Pd(\kappa^1$-*N*-$PhNO)_2(CNAr^{Dipp2})_2$ (1a): Identification of an Equilibrium between Bis-Nitroxide 1a and an η^2-*N*,*O*-Metalloxaziridine Complex. While the solid-state structure of $Pd(\kappa^1$-*N*-$PhNO)_2$-$(CNAr^{Dipp2})_2$ (**1a**) is established by X-ray crystallography and combustion analysis, as noted above, preliminary observations of its spectroscopic signatures in solution were inconsistent with its established magnetic properties.[52] Dissolution of forest green crystals of $Pd(\kappa^1$-*N*-$PhNO)_2(CNAr^{Dipp2})_2$ (**1a**) in benzene-d_6 or deuterated tetrahydrofuran (THF-d_8) produces a deep red solution. Analysis by ^{1}H and $^{13}C\{^1H\}$ NMR spectroscopy reveals the prominence of diamagnetic species in solution, with only one Ar^{Dipp2} environment apparent. This observation is inconsistent with the presence of $Pd(\kappa^1$-*N*-$PhNO)_2(CNAr^{Dipp2})_2$ (**1a**) in solution, as its thermally accessible triplet state would be reasonably expected to produce paramagnetically shifted and broadened NMR spectra.[62,63] Evans method measurements (C_6D_6, 20 °C) failed to detect any significant magnetic moment in these solutions, suggesting that very little of the diradical $Pd(\kappa^1$-*N*-$PhNO)_2(CNAr^{Dipp2})_2$ (**1a**) is present in solution under these conditions. The FTIR spectra of these solutions show two strong ν(C≡N) absorbances at 2146 and 2115 cm^{-1} (Figure 1), as well as

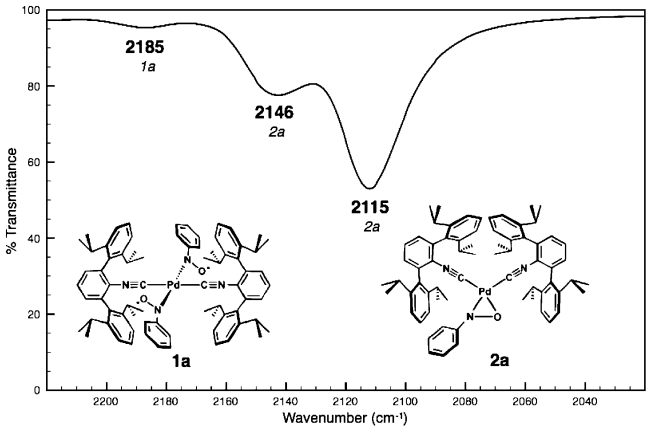

Figure 1. Solution FTIR spectrum (C_6D_6, 20 °C, ν(C≡N) region) of a solution prepared from a crystalline sample of *trans*-$Pd(\kappa^1$-*N*-$PhNO)_2(CNAr^{Dipp2})_2$ (**1a**).

the ν(N═O) stretch of free nitrosobenzene (1506 cm^{-1}). The ν(C≡N) bands are of similar energy and relative intensity to those displayed by $Pd(\eta^2$-*N*,*O*-*o*-Me-$C_6H_4NO)(CNAr^{Dipp2})_2$,[52] thereby suggesting that the predominant complex in solution is the η^2-*N*,*O* mononitrosobenzene metalloxaziridine complex $Pd(\eta^2$-*N*,*O*-PhNO$)(CNAr^{Dipp2})_2$ (**2a**). An independent synthesis of the metalloxaziridine $Pd(\eta^2$-*N*,*O*-PhNO$)(CNAr^{Dipp2})_2$ (**2a**, Scheme 1 and Figure 2) was achieved upon the addition of an equimolar amount of nitrosobenzene to $Pd(CNAr^{Dipp2})_2$ followed by crystallization from an *n*-pentane/hexamethyldisiloxane ($(Me_3Si)_2O$) mixture. As expected, pure samples of $Pd(\eta^2$-*N*,*O*-PhNO$)(CNAr^{Dipp2})_2$ (**2a**) produce identical NMR and FTIR spectroscopic features as do solutions prepared from solid samples of $Pd(\kappa^1$-*N*-$PhNO)_2(CNAr^{Dipp2})_2$ (**1a**), thus

DOI: 10.1021/acs.inorgchem.5b01252
Inorg. Chem. 2015, 54, 7110−7121

Scheme 1. Reactivity of Pd(CNAr^{Dipp2})$_2$ with 1 and 2 Equiv of Nitrosobenzene

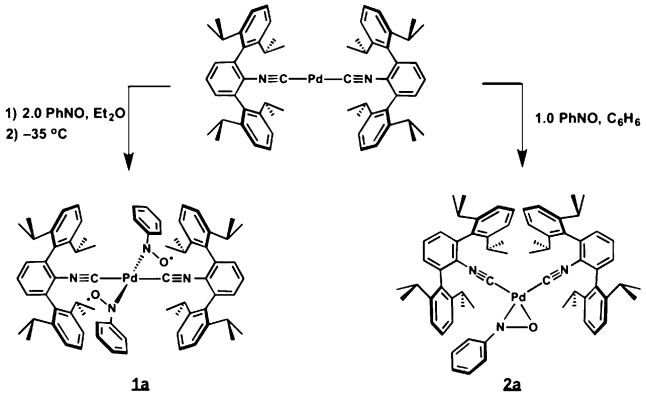

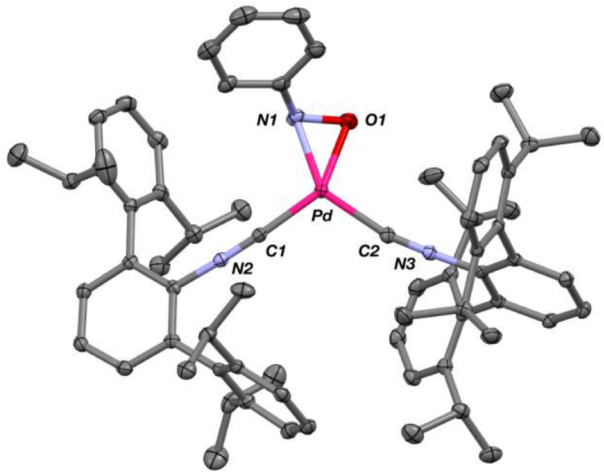

Figure 2. Molecular structure of Pd(η^2-*N,O*-PhNO)(CNAr^{Dipp2})$_2$ (**2a**). Selected bond distances (Å) and angles (deg): N1–O1 = 1.349(3); Pd–N1 = 2.072(2); Pd–O1 = 2.037(2); Pd–C1 = 1.985(2); Pd–C2 = 2.033(2); C1–Pd–N1 = 109.21(8); C2–Pd–O1 = 103.56(8); C1–Pd–C2 = 108.61(9).

confirming that the latter undergoes nitrosobenzene dissociation to produce **2a** in solution. Accordingly, as suspected, the NMR spectroscopic data reported for **1a**,[49] which were indicative of a diamagnetic compound, correspond in fact to that of the metalloaziridine **2a**.

In the solid state, complex **2a** features a N–O bond distance of 1.349(3) Å, which is elongated relative to those in Pd(κ^1-*N*-PhNO)$_2$(CNAr^{Dipp2})$_2$ (**1a**; *d*(N–O) = 1.291(2) Å).[49] However, the N–O bond distance in **2a** is comparable to that in Pd(η^2-*N,O*-*o*-TolNO)(CNAr^{Dipp2})$_2$ (*d*(N–O) = 1.364(4) Å),[52] lending credence to a description of **2a** as bearing a doubly reduced nitrosobenzene ligand supported by a divalent Pd center. Notably, the values of *d*(N–O) for Pd(η^2-*N,O*-PhNO)(CNAr^{Dipp2})$_2$ (**2a**) and Pd(η^2-*N,O*-*o*-TolNO)-(CNAr^{Dipp2})$_2$ are the shortest reported among structurally characterized mononuclear metalloaziridines[64−68] and are somewhat shorter than expected for a N–O single bond.[33] However, we have shown that this discrepancy can be ascribed to a high degree of covalency in the η^2-*N,O* interaction between the Pd center and the nitroso unit as computed for Pd(η^2-*N,O*-*o*-TolNO)(CNAr^{Dipp2})$_2$.[52] Corroborating this notion for **2a** is the presence of isocyanide ν(C≡N) stretching frequencies (2146, 2115 cm^{-1}) that, while higher in energy than those seen for Pd(CNAr^{Dipp2})$_2$, are considerably red-shifted relative to those of the isovalent η^2-peroxo complex Pd(η^2-O$_2$)-(CNAr^{Dipp2})$_2$ (2175, 2149 cm^{-1}).[49]

The formation of metalloaziridine **2a** and free PhNO upon dissolution of crystalline bis-nitroxide **1a** suggested the presence of an equilibrium between these species, with **2a** being overwhelmingly favored at higher temperatures (Scheme 2). Notably, attempts to observe Pd(κ^1-*N*-PhNO)$_2$(CNAr^{Dipp2})$_2$ (**1a**) at lower temperatures in this mixture by variable-temperature ^{1}H NMR spectroscopy proved unsuccessful, as the combined effects of the compound's paramagnetism, low abundance in solution, and the presence of free PhNO precluded an unambiguous assignment of its resonances. However, room-temperature FTIR spectra of C$_6$D$_6$ solutions originating from crystalline **1a** revealed a very weak absorbance at 2185 cm^{-1} (Figure 1). This band closely matches the ν(C≡N) band observed in the solid-state FTIR spectra obtained from crystalline **1a** (2188 cm^{-1}, KBr pellet), thereby indicating that detectable quantities of Pd(κ^1-*N*-PhNO)$_2$(CNAr^{Dipp2})$_2$ (**1a**) are present in solution at room temperature. In addition, variable-temperature FTIR studies in toluene revealed that this band becomes more pronounced with decreasing temperature (Figure 3), which provides strong support for an equilibrium between **1a**, **2a**, and PhNO in solution. However, it is critical to note that even at −80 °C in toluene solution, metalloaziridine **2a** remains the predominant isocyanide-containing component of the mixture (Figure 3). Therefore, we contend that the ability to isolate crystalline Pd(κ^1-*N*-PhNO)$_2$(CNAr^{Dipp2})$_2$ (**1a**) in good yields (60–70%) when a 2:1 PhNO/Pd(CNAr^{Dipp2})$_2$ ratio is employed stems from its high crystallinity, which results in selective precipitation from ethereal solutions. Importantly, the ability of trans-spanning *m*-terphenyl isocyanides to induce the selective crystallization of minor components of an equilibrium mixture has been reported previously for cobalt–carbonyl

Scheme 2. Equilibrium between Bis-nitroxide Diradical 1a and Metalloaziridine 2a

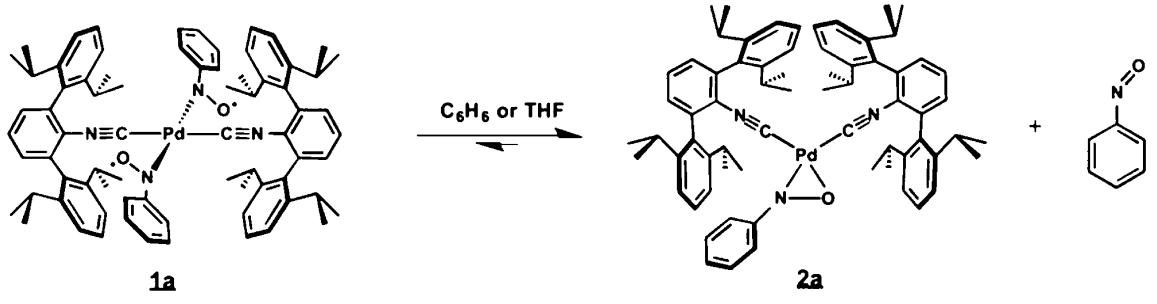

DOI: 10.1021/acs.inorgchem.5b01252
Inorg. Chem. 2015, 54, 7110–7121

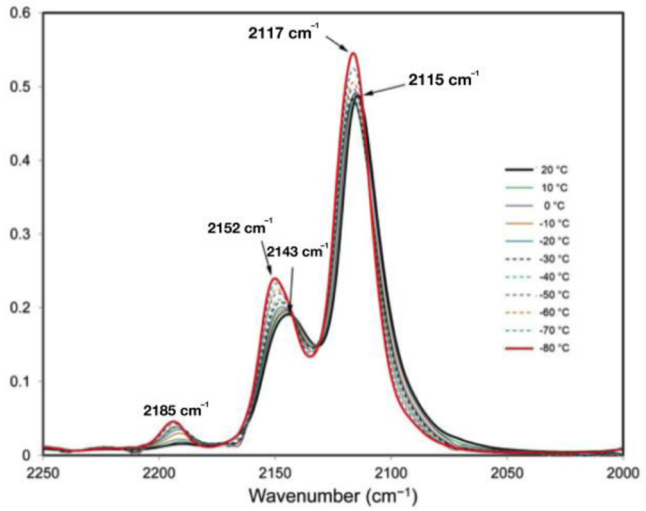

Figure 3. Variable-temperature FTIR spectra (ν(C≡N) region; CaF_2 windows) of toluene solutions prepared from crystalline samples of Pd(κ^1-*N*-PhNO)$_2$(CNAr^{Dipp2})$_2$ (**1a**). The peaks ranging from 2143 to 2152 cm^{-1} and 2115−2117 cm^{-1} correspond to Pd(η^2-*N*,*O*-PhNO)-(CNAr^{Dipp2})$_2$ (**2a**), while that seen to grow in at decreasing temperatures and centered at 2185 cm^{-1} is ascribed to Pd(κ^1-*N*-PhNO)$_2$(CNAr^{Dipp2})$_2$ (**1a**).

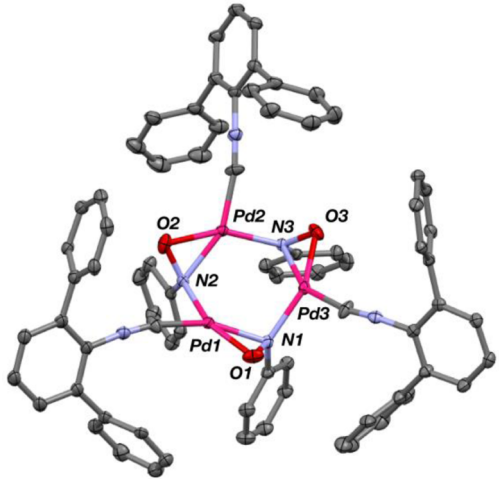

Figure 4. Molecular structure of [Pd(μ^2:η^2-*N*,*O*-η^1-*N*-PhNO)-(CNAr^{Dipp2})]$_3$ (**4**), showing the major component of the modeled positional disorder. Flanking *i*-Pr groups were omitted for clarity.

complexes.[69] Accordingly, this suggestion indicates that there is an inherent kinetic lability of the Pd/κ^1-*N* PhNO-radical linkage in **1a**, which is overcome primarily by lattice formation effects.

In an attempt to chemically drive the equilibrium between **1a** and **2a** toward the bis-nitroxide complex, 5.0 additional equivalents of nitrosobenzene were added to an equilibrated mixture in benzene solution at room temperature. Analysis by FTIR spectroscopy immediately after the addition of excess PhNO indicated the equilibrium between **1a** and **2a** was not significantly altered, further signifying that simple binding of PhNO to **2a** is strongly disfavored at room temperature. However, after ca. 6 h, the presence of excess equivalents of PhNO results in the formation of three new products, with the complete consumption of both **1a** and **2a**. Analysis by ^{1}H NMR, FTIR, GC-MS, and X-ray crystallography indicated that the organic isocyanate, OCNAr^{Dipp2} (**3**), and azoxybenzene (i.e., PhN═N(O)Ph) are produced from this mixture, while the Pd-containing product formed is the cyclic metalloxaziridine trimer [Pd(μ^2:η^2-*N*,*O*-η^1-*N*-PhNO)(CNAr^{Dipp2})]$_3$ (**4**, Figure 4).[70] This process is reminiscent of the production of *tert*-butylisocyanate mediated by the reaction of nitrosobenzene with Ni(*t*-BuNC)$_4$, a transformation in which the isolable mononuclear metalloxaziridine Ni(η^2-*N*,*O*-PhNO)(*t*-BuNC)$_2$ has been proposed as an intermediate.[71] Likewise, we believe that production of OCNAr^{Dipp2} (**3**), azoxybenzene, and trimer **4** may proceed by the mechanism outlined in Scheme 3, whereby an additional equivalent of PhNO inserts into the metalloxaziridine functionality of **2a** followed by oxygen-atom transfer and elimination of the weakly coordinating isocyanate and azoxybenzene fragments from the palladium center. Similar insertion reactions of unsaturated substrates into late metal metalloxaziridines have been observed previously, with those involving Pt(η^2-*N*,*O*-PhNO)(PPh$_3$)$_2$ being the most well-studied.[64,72−74] In addition, the formation of the trinuclear metalloxaziridine complex **4** can be rationalized by trapping of a resultant monoligated [Pd(CNAr^{Dipp2})] species by free PhNO and subsequent trimerization.[75] Most importantly, however, the formation of OCNAr^{Dipp2} (**3**), azoxybenzene, and trimer **4** highlights that an additional process significantly competes with the simple formation of bis-nitroxide complex **1a** from free nitrosobenzene and metalloxaziridine **2a**.

Formation and Solution-Phase Behavior of Pd Bis-Nitroxide Diradicals Featuring Monosubstituted Aryl Groups. To address the dissociation of PhNO from the Pd center in **1a** and access a kinetically persistent bis-nitroxide diradical complex, we sought to modify the electronic profile of the nitrosoarene framework. While the introduction of electron-releasing substituents on the aryl ring may be expected to result in more effective σ-donation of the nitrosoarene ligand to a palladium center, it is important to note that such substituents also decrease the reduction potential of the ArNO unit.[76,77] Correspondingly, electron-withdrawing substituents, which may be expected to promote N═O bond reduction, will also diminish the σ-donor abilities of the ArNO ligand. Therefore, we surveyed a range of electronically varied nitrosoarenes to determine if a balance between σ-donation and N═O bond reduction could be found and promote the generation of a solution-phase persistent bis-nitroxide diradical complex.

As shown in Scheme 4, the synthesis of palladium bis-nitroxide diradical complexes is indeed general and is not exclusively limited to nitrosobenzene. Accordingly, treatment of 0.5 equiv of Pd(CNAr^{Dipp2})$_2$ in Et$_2$O with nitrosoarenes bearing *m*/*p*-chloro, *m*/*p*-bromo, *p*-fluoro, *m*/*p*-methyl, *p*-phenyl, or *m*-formyl substitution patterns readily provides the bis-nitroxide diradical complexes *trans*-Pd(κ^1-*N*-ArNO)$_2$(CNAr^{Dipp2})$_2$ (**1b**−**j**) upon crystallization at −35 °C. However, it is notable that the strongly donating nitrosoarenes *p*-Me$_2$NC$_6$H$_4$NO or *p*-MeOC$_6$H$_4$NO, for which a dipolar quinonoid form is a major resonance contributor (Scheme 5), do not react with Pd(CNAr^{Dipp2})$_2$ over the course of days at room temperature. This lack of reactivity of nitrosoarenes featuring strongly electron-releasing substituents indicates that N═O bond reduction is a critical kinetic component to the formation of bis-nitroxide species, as the quinonoid form of such strongly donating nitrosoarenes is also expected to inhibit the formation of η^2-*N*,*O* metalloxaziridine complexes.[33] Crystallographic characterization of complexes **1b**−**j** revealed a trans, anti-

DOI: 10.1021/acs.inorgchem.5b01252
Inorg. Chem. 2015, 54, 7110−7121

Scheme 3. Proposed Mechanism Leading to the Formation of Azoxybenzene, $OCNAr^{Dipp2}$ (3), and $[Pd(\mu^2{:}\eta^2{-}N,O{-}\eta^1{-}N{-}PhNO)(CNAr^{Dipp2})]_3$ (4)

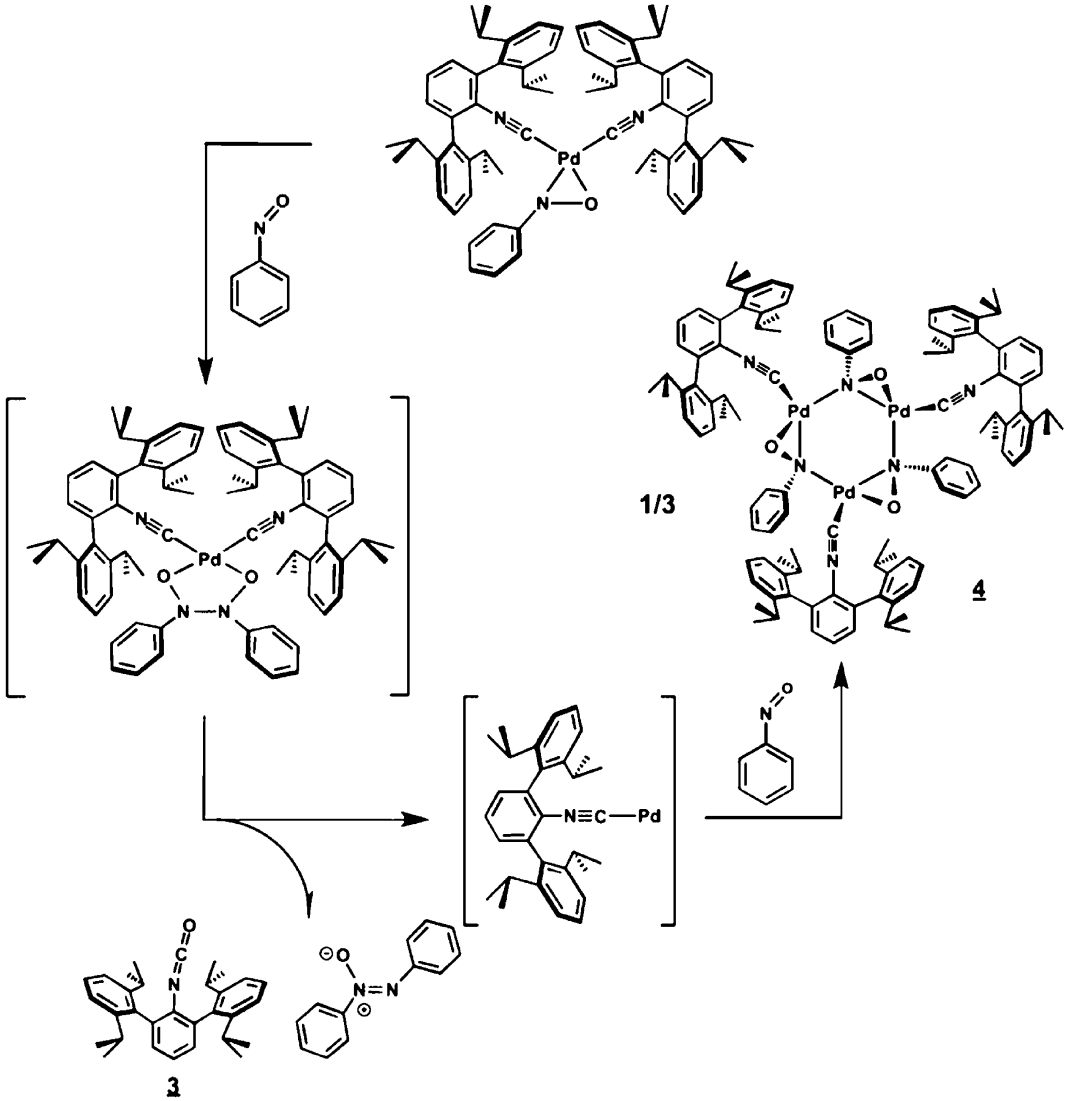

disposition of the nitroxide groups about a square planar Pd center, resulting in approximate C_{2h} site symmetry in a manner identical to the parent bis-nitroxide complex **1a** (Figure 5).[78] The N−O bond lengths in complexes **1b−j** range from 1.256(3) to 1.288(3) Å (Table 1) and are consistent with a singly reduced nitroxide radical description.[52] Correspondingly, the Pd−C_{iso} distances are significantly elongated relative to those seen in $Pd(CNAr^{Dipp2})_2$ (1.930(4) Å),[49] indicative of decreased backbonding to the isocyanide ligands as a result of an increase in formal oxidation state of the Pd center. The solid-state FTIR spectra (KBr pellet) of **1b−j** corroborate this description and feature high-energy ν(C≡N) stretches (2180−2196 cm^{-1}; Table 1).

Whereas bis-nitroxide complexes **1b−j** can be readily isolated and characterized in the solid state, they all display solution-phase behavior similar to that of the parent diradical **1a**. Accordingly, dissolution of crystalline samples of **1b−j** in arene or ethereal solvents results in the rapid dissociation of one nitrosoarene ligand to produce the η^2-*N,O* metalloaziridine complexes **2b−j** and free nitrosoarene as assayed by solution FTIR, ^{1}H NMR, and $^{13}C\{^1H\}$ NMR spectroscopy. The metalloaziridines **2b−j** could be independently generated by treatment of $Pd(CNAr^{Dipp2})_2$ with 1 equiv of the corresponding nitrosoarene (Scheme 4). As with $Pd(\eta^2$-*N,O*-PhNO)-$(CNAr^{Dipp2})_2$ (**2a**), the solution FTIR spectra of **2b−j** display two diagnostic ν(C≡N) bands in the 2100−2160 cm^{-1} region (Table 2). In addition, crystallographic characterization of complexes **2b−j** (Figure 6) revealed N−O bond lengths (1.334(3)−1.354(7) Å; Table 2) similar to that found in $Pd(\eta^2$-*N,O*-PhNO)$(CNAr^{Dipp2})_2$ (**2a**) and consistent with an η^2-*N,O* metalloaziridine formulation.[79] Most importantly, however, for the arene substitution patterns represented by complexes **1b−j**, there is no apparent inhibition of nitrosoarene dissociation that leads to reasonable solution-phase persistence.

In contrast, the specific use of either *para*-formyl (*p*-CHO) or *para*-cyano (*p*-CN) nitrosobenzene leads to bis-nitroxide Pd complexes that show marked persistence in solution. Accordingly, treatment of 0.5 equiv of $Pd(CNAr^{Dipp2})_2$ with either (*p*-CHO)C_6H_4NO or (*p*-CN)C_6H_4NO in Et_2O at room temperature generates the bis-nitroxide diradicals $Pd(\kappa^1$-*N*-*p*-$C(O)H$-$C_6H_4NO)_2(CNAr^{Dipp2})_2$ (**1k**) and $Pd(\kappa^1$-*N*-*p*-CN-$C_6H_4NO)_2(CNAr^{Dipp2})_2$ (**1l**), respectively. Unlike complexes

DOI: 10.1021/acs.inorgchem.5b01252
Inorg. Chem. 2015, 54, 7110−7121

Scheme 4. Formation of 1b–l and 2b–l from $Pd(CNAr^{Dipp2})_2$ and Monosubstituted Nitrosoarenes

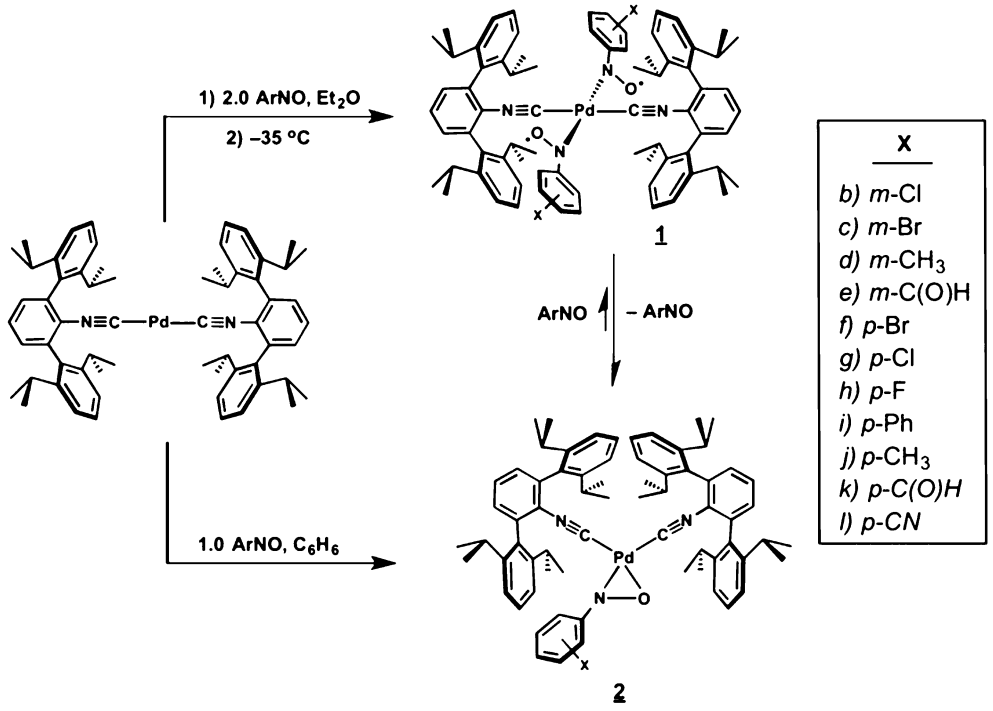

Scheme 5. Quinonoid Resonance Structure of Nitrosoarenes Bearing Para-Oriented Electron Releasing Groups As Exemplified by 4-(Dimethylamino)nitrosobenzene

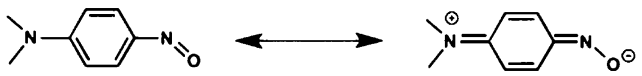

1a–j, both **1k** and **1l** readily precipitate from the reaction mixture upon formation and can be isolated as dark purple (**1k**) or green (**1l**) microcrystalline solids, respectively, in good yields (ca. 70%). Crystallographic characterization of **1k** and **1l** (Figures 7 and 8) on single crystals obtained from cooling dilute Et_2O/THF solutions to −35 °C reveals square planar Pd centers and N–O bond lengths indicative of nitroxide radical ligands (d(N–O) = 1.275(4) Å (**1k**) and 1.275(3) Å (**1l**); Table 1). Most importantly, the solution-phase properties of **1k** and **1l** are consistent with a significant retention of their bis-nitroxide radical formulation. For example, solution FTIR spectra of **1k** and **1l** in THF or C_6D_6 revealed intense ν(C≡N) bands centered at 2190 cm^{-1} consistent with the presence of $Pd(\kappa^1\text{-}N\text{-ArNO})_2(CNAr^{Dipp2})_2$ bis-nitroxide complexes (Figure 9). While ν(C≡N) bands attributable to the corresponding metalloaziridines **2k** and **2l** are also present in these spectra, the fact that these are not the dominant species stands in stark contrast to the solution-phase behavior of the bis-nitroxide complexes **1a–j**. In addition, the ^{1}H NMR spectra of *para*-formyl **1k** and *para*-cyano **1l** in C_6D_6 feature broad and shifted resonances indicative of the presence of paramagnetic species. These solutions give rise to measurable solution-phase magnetic moments of ca. 1.9 μ_B (Evans method, 20 °C),[80] which, when compared to the negligible magnetic moment observed for C_6D_6 solutions originating from complexes **1a–j**, provide further indication for the existence of paramagnetic species in solution.

It is important to note that, while spectroscopically observable by both ^{1}H NMR and IR spectroscopy, the metalloaziridines **2k** and **2l** are not readily isolated in pure form. Indeed, treatment of $Pd(CNAr^{Dipp2})_2$ with 1.0 equiv of either *para*-formyl or *para*-cyano nitrosobenzene leads to the formation of a mixture of metalloaziridine and bis-nitroxide complexes, as well as unreacted $Pd(CNAr^{Dipp2})_2$. Furthermore, the metalloaziridines **2k** and **2l** do not selectively deposit from these mixtures by crystallization. Accordingly, we believe the production of these mixtures suggests that the bis-nitroxide complexes are formed rapidly in solution and that a kinetic barrier to ArNO dissociation arises when either *para*-formyl or *para*-cyano substituents are present on the aryl ring. It is also critical to note that room-temperature solutions of **1k** and **1l** are observed to only slowly become enriched in the metalloaziridines **2k** and **2l**, with the presence of $OCNAr^{Dipp2}$ (**3**) and azoxyarenes also becoming evident (see Supporting Information, Figures S2.1 and S2.2), thus demonstrating a retardation of the analogous equilibrium and insertion chemistry that was observed for the parent diradical **1a**. This observation further serves to highlight an apparent decrease in the lability of a nitroxide ligand in **1k–l** as a result of the installation of *para*-formyl and *para*-cyano substituents.

Origin of the Solution-Phase Persistence of *para*-Cyano and *para*-Formyl Bis-arylnitroxide Radical Complexes. It is evident from the results above that the solution-phase kinetic persistence of $Pd(\kappa^1\text{-}N\text{-ArNO})_2(CNAr^{Dipp2})_2$ bis-nitroxide complexes is sensitive to very specific electronic modulations of the nitrosoarene framework. This suggestion is highlighted by the marked differences in the solution-phase properties between complexes **1a–j** and **1k–l** but also more directly between complexes **1e** and **1k**, which feature *meta*-formyl and *para*-formyl substituents, respectively. To account for this dichotomy, it is important to note that *para*-oriented electron-releasing groups, such as $-NMe_2$ (Hammett σ = −0.88),[81] are known to increase the Lewis basicity, and

DOI: 10.1021/acs.inorgchem.5b01252
Inorg. Chem. 2015, 54, 7110–7121

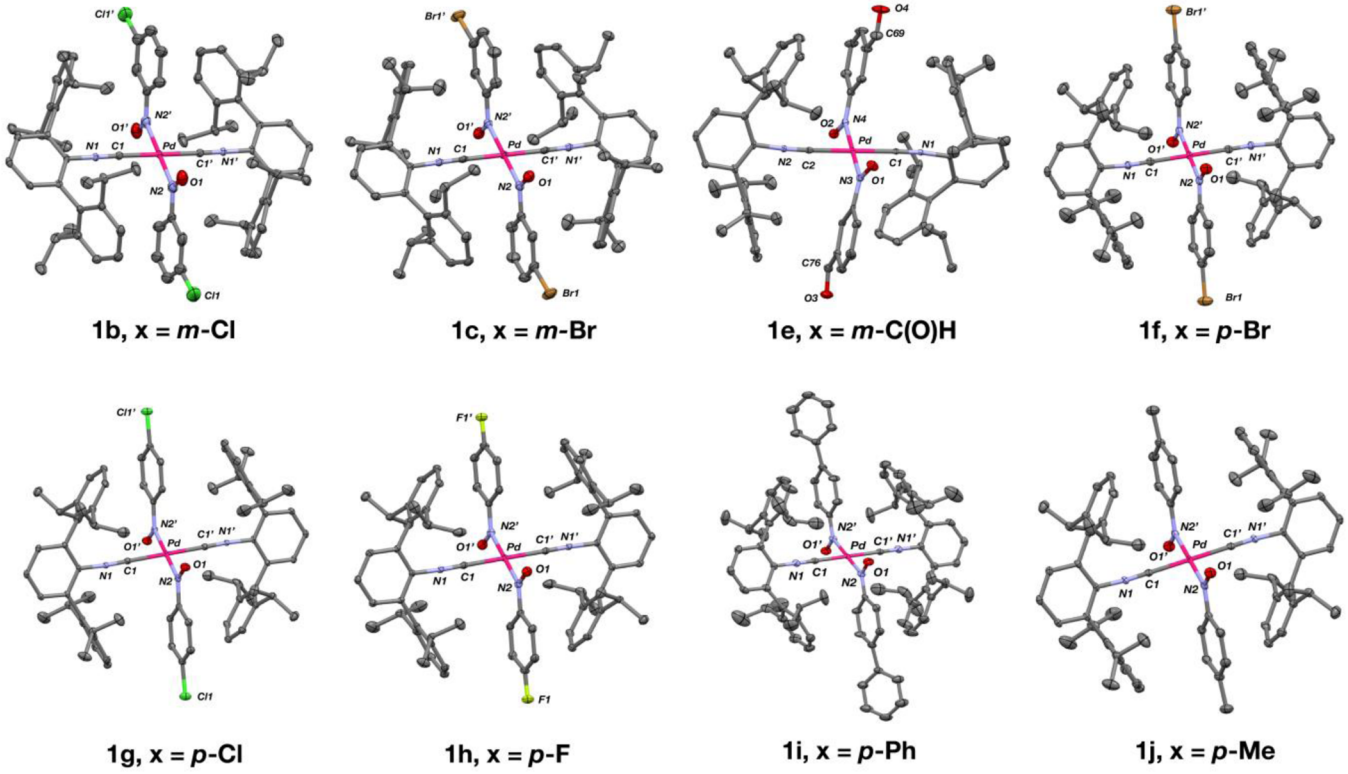

Figure 5. Molecular structures of $Pd(\kappa^1\text{-}N\text{-}ArNO)_2(CNAr^{Dipp2})_2$ (**1b,c** and **e–j**).

Table 1. Nitrosoarene N–O Bond Lengths and Isocyanide Stretching Frequencies for Complexes 1a–l in the Solid State

complex (substituent)	nitrosoarene d(N–O) (Å)	isocyanide ν(C≡N) (cm^{-1})[a]
1a (H)[b]	1.291(2)	2185
1b (*m*-Cl)	1.267(6)	2185
1c (*m*-Br)	1.280(5)	2187
1d (*m*-CH_3)	*c*	2180
1e (*m*-COH)	1.270(4)[d]	2196
1f (*p*-Br)	1.256(3)	2188
1g (*p*-Cl)	1.279(2)	2188
1h (*p*-F)	1.287(3)	2188
1i (*p*-Ph)	1.288(3)	2186
1j (*p*-CH_3)	1.267(3)	2180
1k (*p*-COH)	1.275(4)	2189
1l (*p*-CN)	1.275(3)	2186

[a]KBr pellet. [b]Data from ref 49. [c]Crystallographic positional disorder prevented a precise determination of the N–O bond length in complex **1d**. [d]Average of two crystallographically independent Pd-bound nitrosoarenes. Error is reported as the standard error of the mean.

Table 2. Nitrosoarene N–O Bond Lengths and Isocyanide Stretching Frequencies for Complexes 2a–l in the Solid State

complex (substituent)	nitrosoarene d(N–O) (Å)	isocyanide ν(C≡N) (cm^{-1})[a]
2a (H)	1.349(3)	2149, 2105
2b (*m*-Cl)	1.334(3)	2153, 2111
2c (*m*-Br)	1.341(4)	2155, 2112
2d (*m*-CH_3)	1.349(2)	2148, 2108
2e (*m*-COH)	1.349(3)	2151, 2121
2g (*p*-Cl)	1.354(3)	2150, 2121
2h (*p*-F)	1.35(1)	2145, 2117
2i (*p*-Ph)	*b*	2143, 2114
2j (*p*-CH_3)	1.354(7)	2137, 2117

[a]KBr pellet. [b]Complex **2i** was not crystallographically characterized.

therefore σ-donor abilities, of nitrosoarenes.[35] By analogy, the presence of *para*-formyl ($\sigma = 0.42$) and *para*-cyano ($\sigma = 0.66$)[81] substituents are expected to attenuate σ-donor abilities of nitrosoarenes. Such ligands should therefore display a decreased trans effect and, given the trans disposition of the nitroxide ligands in **1k** and **1l**, might be expected to diminish the prevalence of nitrosoarene dissociation from these species.

However, as a critical point, other bis-nitroxide diradicals in this series bearing substituents with large and positive Hammett σ-values (e.g., *m*-Br $\sigma = +0.39$, *m*-Cl $\sigma = +0.37$)[81] do not exhibit the prolonged kinetic persistence exhibited by **1k** and **1l**. This indicates that an additional electronic effect governs the relative solution-phase stability of complexes **1k** and **1l**. In this regard, it is noteworthy that the presence of electronically unsaturated electron-withdrawing substituents in the para position has been found to significantly increase the reduction potentials of uncoordinated nitrosoarenes.[76,77] Furthermore, inductive-type electron-withdrawing substituents (e.g., F, Cl, Br) have been reported to induce relatively smaller changes in the reduction potentials of the corresponding nitrosoarenes, with para-oriented halogens resulting in decreased potentials relative to that of nitrosobenzene.[76] This finding suggests that electronically unsaturated substituents are capable of efficiently delocalizing spin density to positions exo of the aryl ring, thereby increasing the stability of the arylnitroxide radical. Indeed, for transition metal-bound arylnitroxide radicals, such behavior has been recently observed in a series of ruthenium-

DOI: 10.1021/acs.inorgchem.5b01252
Inorg. Chem. 2015, 54, 7110–7121

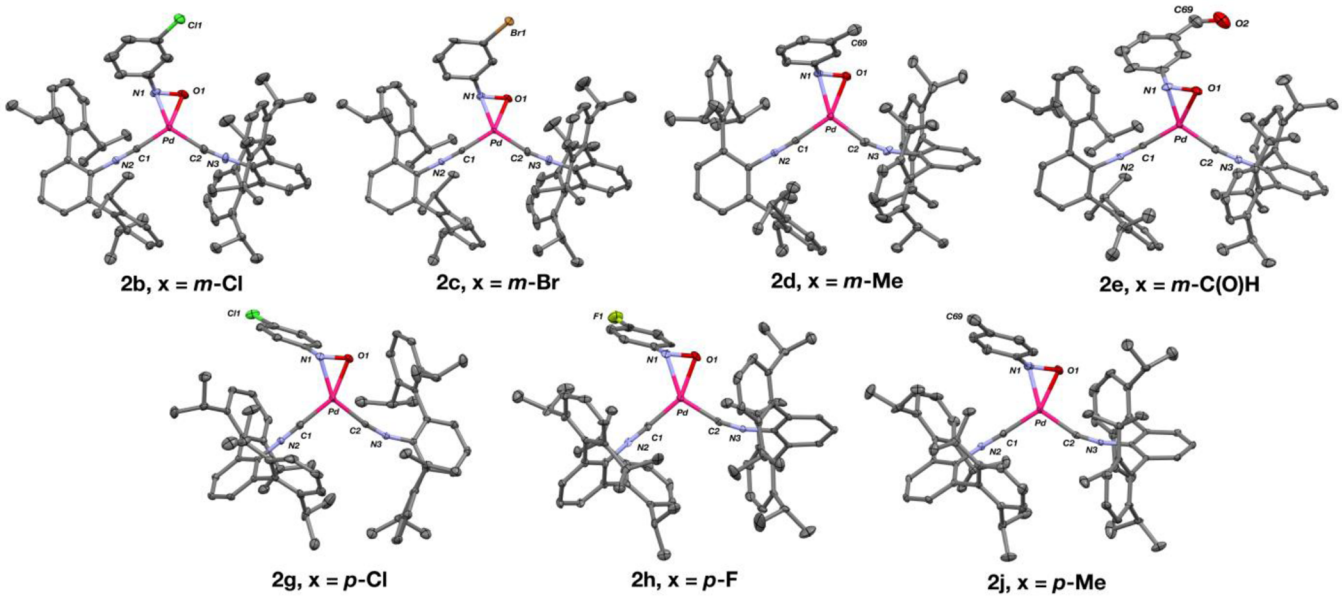

Figure 6. Molecular structures of Pd(η^2-*N,O*-ArNO)$(CNAr^{Dipp2})_2$ (**2b–e**, **g**, **h**, **j**).

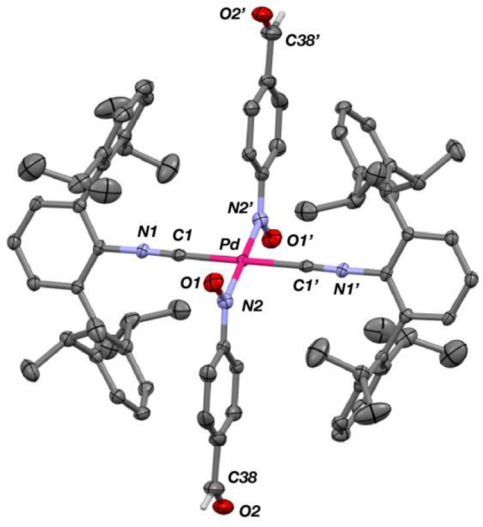

Figure 7. Molecular structure of Pd(κ^1-*N*-*p*-C(O)H-$C_6H_4NO)_2(CNAr^{Dipp2})_2$ (**1k**). Selected bond distances (Å) and angles (deg): N2–O1 = 1.275(4); Pd–N2 = 2.023(3); Pd–C1 = 2.007(4); C1–Pd–N2 = 88.8(1); N2–Pd–C1′: 91.2(1).

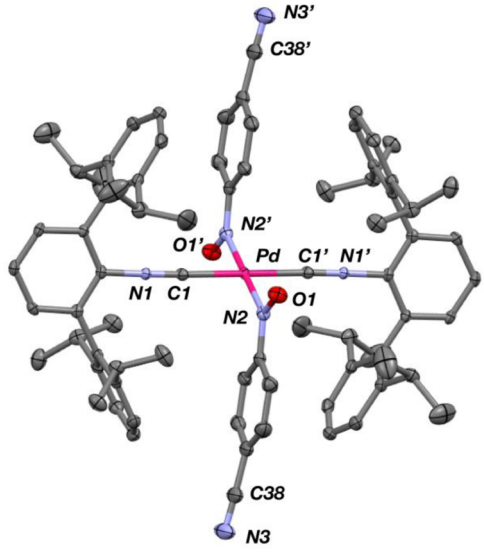

Figure 8. Molecular structure of Pd(κ^1-*N*-*p*-CN-$C_6H_4NO)_2(CNAr^{Dipp2})_2$ (**1l**). Selected bond distances (Å) and angles (deg): N2–O1 = 1.275(3); Pd–N2 = 2.014(3); Pd–C1 = 2.001(3); C1–Pd–N2 = 91.8(1); N2–Pd–C1′: 88.2(1).

(II) complexes supported by chelating 2-(2-nitrosoaryl)-pyridine ligands. In this case, introduction of a nitro (NO_2) group on the nitrosoaryl ring has been found to decrease the spin density on the nitroso –N═O moiety relative to an unsubstituted nitrosoaryl derivative in singly reduced nitroxide complexes.[51] Furthermore, the effect was most pronounced when the nitro group was oriented *para* to the nitroso functionality. Spin-density plots[82] derived from broken-symmetry density functional theory calculations on the model complexes Pd(κ^1-*N*-*p*-C(O)H-$C_6H_4NO)_2(CNPh)_2$ and Pd(κ^1-*N*-*p*-CN-$C_6H_4NO)_2(CNPh)_2$ are consistent with this notion. As shown in Figure 10, a moderate degree of spin delocalization onto the *para*-formyl and *para*-cyano substitutents, respectively, is apparent. These spin-density plots can also be compared to that previously reported for the model complex Pd(κ^1-*N*-$PhNO)_2(CNPh)_2$, which does not possess substituted arylnitroxide ligands and accordingly does not show spin delocalization onto positions exo to the nitrosophenyl ring.[52]

Most importantly, however, experimental evidence for spin delocalization onto the *para*-formyl and *para*-cyano substituents in complexes **1k** and **1l** is apparent in their solution-phase IR spectra and solid-state magnetic susceptibility. For example, in C_6D_6 at room temperature, the formyl ν(C═O) stretch of **1k** is found at 1677 cm^{-1}, which is 16 cm^{-1} lower than that observed for the metalloxaziridine **2k** (1693 cm^{-1}; Supporting Information, Figure S2.1) and 29 cm^{-1} lower than that of free *p*-formylnitrosobenzene (1706 cm^{-1}, THF). As the Pd → (NO π^*) π-backbonding interactions attendant in the η^2-N,O metalloxaziridine complexes are also expected to marginally affect the degree of electron density on the nitrosoaryl unit,[52] we interpret the fact that the *para*-formyl ν(C═O) stretch in

DOI: 10.1021/acs.inorgchem.5b01252
Inorg. Chem. 2015, 54, 7110–7121

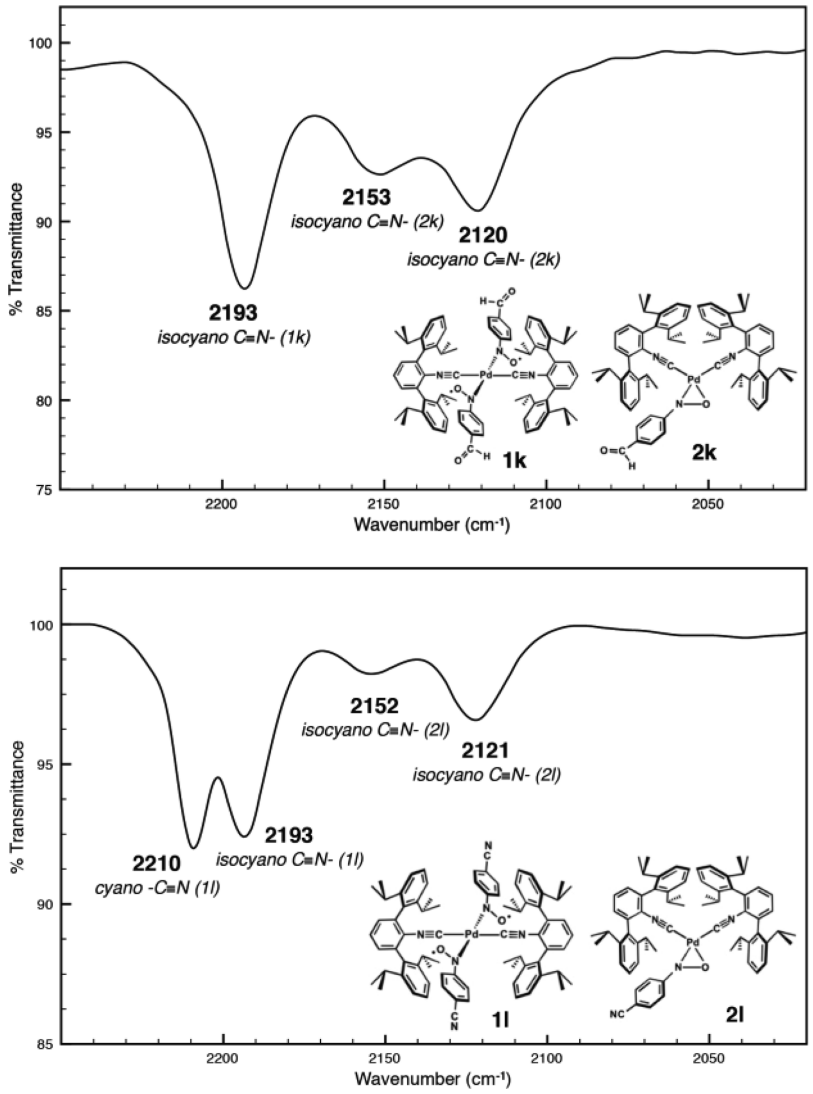

Figure 9. FTIR spectra (ν(C≡N) region) of THF solutions freshly prepared from crystalline samples of Pd(κ^1-*N*-*p*-C(O)H-$C_6H_4NO)_2(CNAr^{Dipp2})_2$ (**1k**, upper) and Pd(κ^1-*N*-*p*-CN-$C_6H_4NO)_2(CNAr^{Dipp2})_2$ (**1l**, lower). Conditions: 20 °C, KBr windows.

1k is of lower energy than that in **2k** as an indication that greater charge/spin delocalization onto the formyl unit is present in the nitroxide radical form of the coordinated nitrosoarene. Similarly, the *para*-cyano ν(C≡N) stretch for bis-nitroxide **1l** (2210 cm^{-1}) is red-shifted relative to that of the metalloxaziridine **2l** (2221 cm^{-1}; Supporting Information, Figure S2.1) and *p*-cyanonitrosobenzene (2232 cm^{-1}, THF), again indicating a greater degree of spin delocalization in the nitroxide radical. In addition, solid-state magnetic susceptibility measurements also provide evidence for spin delocalization onto the *para* substituents in bis-nitroxides **1k** and **1l**. Both **1k** and **1l** display magnetic behavior in the solid state similar to the parent bis-nitroxide **1a**, and the susceptibility curves can be readily fitted to a singlet diradical model ($\hat{H} = -2J \cdot S_1 \cdot S_2$, where $S_1 = S_2 = 1/2$) possessing a thermally accessible triplet ($S = 1$) excited state (Figure 11). However, the antiferromagnetic coupling constants (J) derived for complexes **1k** (J = −89.4 cm^{-1}) and **1l** (J = −88.9 cm^{-1}) are non-negligibly more positive than that of **1a** (J = −115.0 cm^{-1}). This finding indicates that *para*-formyl and *para*-cyano substituents contract the energy difference of the $S = 0$ ground and $S = 1$ excited states of complexes **1k** and **1l** relative to **1a**, likely by lowering the energy of the latter. In effect, these data indicate that *para*-formyl and *para*-cyano groups perturb the electronic structure of these complexes toward a more magnetically uncoupled, spin-isolated nitroxide radical continuum and are consistent with increased spin delocalization over the aryl fragment. For further comparison, it is notable that solid-state magnetic susceptibility measurements on the *para*-chloro derivative **1g** (Supporting Information, Figure S3.1) give rise to an antiferromagnetic coupling constant (J) of −102.5 cm^{-1}. This J value, which is roughly intermediate between that of **1a** and **1k**–**l**, signifies that inductive-type electron-withdrawing groups can increase spin delocalization over the aryl substituent but not to the extent of electronically unsaturated groups such as formyl and cyano.

On the basis of the experimental observations above, we believe that the increased solution-phase persistence of *para*-formyl and *para*-cyano bis-nitroxide complexes **1k** and **1l** originates from the unequal combination of two phenomena. First, attenuation of the trans influence of the nitroxide ligand by introduction of electron-withdrawing groups likely diminishes the extent of dissociation from a metal center. However, this effect is likely minor and specific to these Pd(κ^1-*N*-

DOI: 10.1021/acs.inorgchem.5b01252
Inorg. Chem. 2015, 54, 7110−7121

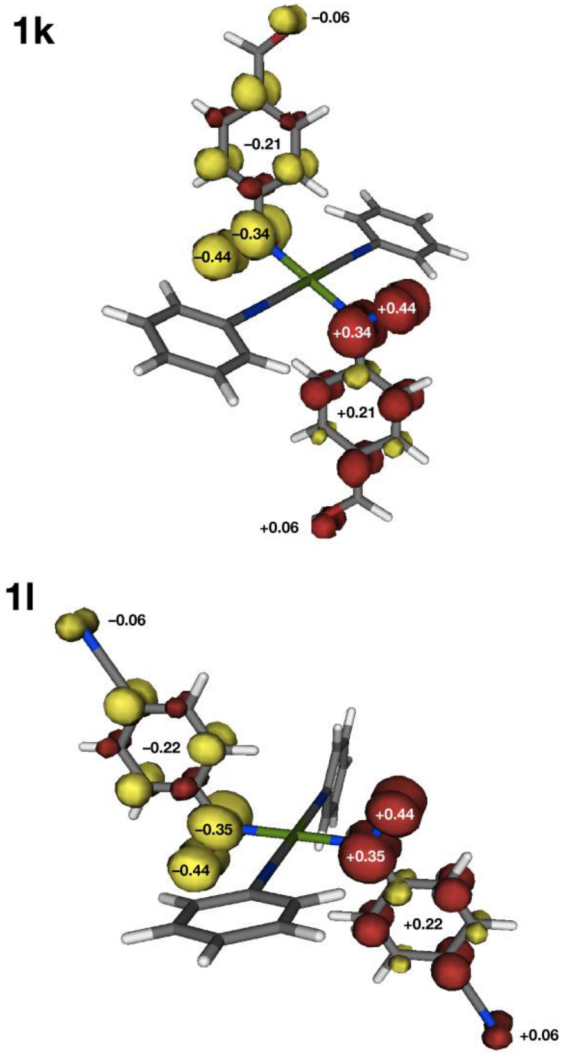

Figure 10. Spin-density plots overlaid with Mulliken spin populations of the BS(1,1) solutions for the model complexes Pd(κ^1-*N*-*p*-C(O)H–$C_6H_4NO)_2(CNPh)_2$ (upper) and Pd(κ^1-*N*-*p*-CN-$C_6H_4NO)_2(CNPh)_2$ (lower). B3LYP, ZORA-def2-TZVP, α-spin in red, β-spin in yellow.

$ArNO)_2(CNAr^{Dipp2})_2$ complexes, where two nitroxide radical ligands are trans oriented. More generally, the ability to increasingly delocalize spin of an aryl nitroxide radical away from the NO unit significantly promotes the kinetic stabilization of such species. Implicit within this suggestion is that an inherent instability of aryl nitroxide radicals exists, which is reasonably supported by the fact that there are limited reports on the isolation of either free *C*-organonitroxide radical anions (i.e., $[RNO]^-$) or monodentate *C*-organonitroxide radical complexes, despite decades of study. Accordingly, as shown here for arylnitroxide ligands, incorporation of electronically unsaturated functional groups para to the NO unit serves as an effective strategy for stabilizing monodentate, metal-coordinated nitroxide radicals and allows for more systematic studies of their chemical and physical properties in both solution and the solid-state.

CONCLUSIONS

In this report, we have demonstrated the significant kinetic lability of a nitrosobenzene ligand in the bis-nitroxide radical complex Pd(κ^1-*N*-PhNO)$_2$($CNAr^{Dipp2}$)$_2$ (**1a**), which has allowed its solid-state and solution-phase properties to be reconciled. The solution-phase equilibrium established between complex **1a**, free nitrosobenzene (PhNO), and the η^2-*N*,*O* metalloaziridine Pd(η^2-*N*,*O*-PhNO)($CNAr^{Dipp2}$)$_2$ (**2a**), along with the fact that the presence of excess PhNO leads to competitive side reactions, indicates that formation of persistent bis-nitroxide radicals in this system is a tenuous occurrence. These observations highlight an inherent solution-phase instability of monodentate, metal-coordinated arylnitroxide radicals, which is not readily overcome by electronic modification of the nitrosoarene framework. However, the specific use of electronically unsaturated electron-withdrawing substituents, which possess diminished trans-effect ability, but more importantly are able to delocalize spin density away from the arylnitroxide NO unit, induces a kinetic barrier to nitrosarene dissociation and promotes the persistence of coordinated nitroxide radicals in solution. We envision that these findings will aid in the development of systems targeting explorations of the chemical and physical properties of metal-coordinated nitroxide radicals. Importantly, they also represent an additional tool for studies aimed at trapping transition metal or other unstable $S = 1/2$ radicals in solution.

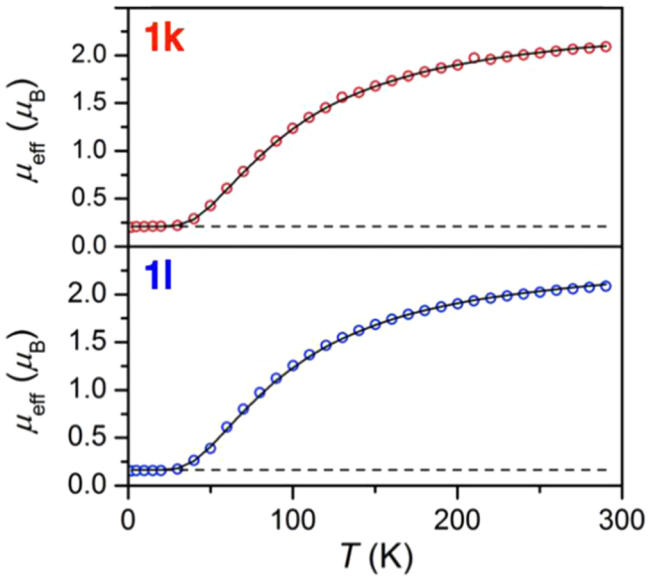

Figure 11. Variable-temperature SQUID data (○) and simulation (line) for Pd(κ^1-*N*-*p*-C(O)H-$C_6H_4NO)_2(CNAr^{Dipp2})_2$ (**1k**) and Pd(κ^1-*N*-*p*-CN-$C_6H_4NO)_2(CNAr^{Dipp2})_2$ (**1l**). Data for both samples were simulated as an antiferromagnetically coupled singlet diradical. Simulation parameters for **1k**: $J = -89.4$ cm^{-1}; paramagnetic impurity = 1.5%; Mol. weight = 1300 g/mol; $\chi_{dia} = -675 \times 10^{-6}$ emu. Simulation parameters for **1l**: $J = -88.9$ cm^{-1}; paramagnetic impurity = 0.9%; Mol. weight = 1320 g/mol; $\chi_{dia} = -800 \times 10^{-6}$ emu.

ASSOCIATED CONTENT

Supporting Information

Synthetic procedures, FTIR spectra, SQUID magnetometry data, and computational and crystallographic details (PDF and CIF). The Supporting Information is available free of charge on the ACS Publications website at DOI: 10.1021/acs.inorgchem.5b01252.

AUTHOR INFORMATION

Corresponding Author

*E-mail: jsfig@ucsd.edu.

DOI: 10.1021/acs.inorgchem.5b01252
Inorg. Chem. 2015, 54, 7110–7121

Notes

The authors declare no competing financial interest.

■ ACKNOWLEDGMENTS

We are grateful to the U.S. National Science Foundation for support of this research (CHE-0954710) and Graduate Research Fellowships to B.R.B. and L.A.L. J.S.F is a Camille Dreyfus Teacher−Scholar (2012-2017). Prof. Clifford P. Kubiak is thanked for access to VT-IR instrumentation, and Profs. William C. Trogler and Jeffrey D. Rinehart are thanked for helpful discussions.

■ REFERENCES

(1) Kaim, W. *Inorg. Chem.* **2011**, *50*, 9752−9765.
(2) Pierpont, C. G. *Coord. Chem. Rev.* **2001**, *216*−*217*, 99−125.
(3) Griffith, W. P. *Transition Met. Chem.* **1993**, *18*, 250−256.
(4) Beswick, C. L.; Schulman, J. M.; Stiefel, E. I. *Prog. Inorg. Chem.* **2003**, *52*, 55−110.
(5) Hine, F. J.; Taylor, A. J.; Garner, C. D. *Coord. Chem. Rev.* **2010**, *254*, 1570−1579.
(6) Eisenberg, R.; Gray, H. B. *Inorg. Chem.* **2011**, *50*, 9741−9751.
(7) Chirik, P. J.; Wieghardt, K. *Science* **2010**, *327*, 794−795.
(8) Bart, S. C.; Lobkovsky, E. L.; Chirik, P. J. *J. Am. Chem. Soc.* **2004**, *126*, 13794−13807.
(9) Tondreau, A. M.; Atienza, C. C. H.; Weller, K. J.; Nye, S. A.; Lewis, K. M.; Delis, J. G. P.; Chirik, P. J. *Science* **2012**, *335*, 567−570.
(10) Luca, O. R.; Crabtree, R. H. *Chem. Soc. Rev.* **2013**, *42*, 1440−1459.
(11) Zhu, D.; Thapa, I.; Korobkov, I.; Gambarotta, S.; Budzelaar, P. H. M. *Inorg. Chem.* **2011**, *50*, 9879−9887.
(12) Knijnenburg, Q.; Gambarotta, S.; Budzelaar, P. H. M. *Dalton Trans.* **2006**, 5442−5448.
(13) Blackmore, K. J.; Ziller, J. W.; Heyduk, A. F. *Inorg. Chem.* **2005**, *44*, 5559−5561.
(14) Lu, C. C.; Bill, E.; Weyhermüller, T.; Bothe, E.; Wieghardt, K. *Inorg. Chem.* **2007**, *46*, 7880−7889.
(15) Dunn, T. J.; Webb, M. I.; Hazin, K.; Verma, P.; Wasinger, E. C.; Shimazaki, Y.; Storr, T. *Dalton Trans.* **2013**, *42*, 3950.
(16) Kaim, W. *Eur. J. Inorg. Chem.* **2012**, 343−348.
(17) Heyduk, A. F.; Zarkesh, R. A.; Nguyen, A. I. *Inorg. Chem.* **2011**, *50*, 9849−9863.
(18) Praneeth, V. K. K.; Ringenberg, M. R.; Ward, T. R. *Angew. Chem., Int. Ed.* **2012**, *51*, 10228−10234.
(19) Lyaskovskyy, V.; de Bruin, B. *ACS Catal.* **2012**, *2*, 270−279.
(20) Valentine, J. S. *Chem. Rev.* **1973**, *73*, 235−245.
(21) Cramer, C. J.; Tolman, W. B. *Acc. Chem. Res.* **2007**, *40*, 601−608.
(22) Jørgensen, C. *Coord. Chem. Rev.* **1966**, *1*, 164−178.
(23) Hayton, T. W.; Legzdins, P.; Sharp, W. B. *Chem. Rev.* **2002**, *102*, 935−991.
(24) Ford, P. C.; Lorkovic, I. M. *Chem. Rev.* **2002**, *102*, 993−1017.
(25) McCleverty, J. A. *Chem. Rev.* **2004**, *104*, 403−418.
(26) Farmer, P. J.; Sulc, F. *J. Inorg. Biochem.* **2005**, *99*, 166−184.
(27) Fukuto, J. M.; Bartberger, M. D.; Dutton, A. S.; Paolocci, N.; Wink, D. A.; Houk, K. N. *Chem. Res. Toxicol.* **2005**, *18*, 790−801.
(28) Weiss, J. J. *Nature* **1964**, *202*, 83−84.
(29) Pauling, L. *Nature* **1964**, *203*, 182−183.
(30) Chen, H.; Ikeda-Saito, M.; Shaik, S. *J. Am. Chem. Soc.* **2008**, *130*, 14778−14790.
(31) Wanat, A.; Schneppensieper, T.; Stochel, G.; van Eldik, R.; Bill, E.; Wieghardt, K. *Inorg. Chem.* **2002**, *41*, 4−10.
(32) Kaim, W.; Schwederski, B. *Coord. Chem. Rev.* **2010**, *254*, 1580−1588.
(33) Lee, J.; Chen, L.; West, A. H.; Richter-Addo, G. B. *Chem. Rev.* **2002**, *102*, 1019−1065.
(34) Gowenlock, B. G.; Richter-Addo, G. B. *Chem. Rev.* **2004**, *104*, 3315−3340.
(35) Cameron, M.; Gowenlock, B. G.; Vasapollo, G. *Chem. Soc. Rev.* **1990**, *19*, 355−379.
(36) Mansuy, D.; Battioni, P.; Chottard, J.-C.; Riche, C.; Chiaroni, A. *J. Am. Chem. Soc.* **1983**, *105*, 455−463.
(37) Muccigrosso, D. A.; Jacobson, S. E.; Apgar, P. A.; Mares, F. *J. Am. Chem. Soc.* **1978**, *100*, 7063−7065.
(38) Askari, M. S.; Girard, B.; Murugesu, M.; Ottenwaelder, X. *Chem. Commun.* **2011**, *47*, 8055−8057.
(39) Hoard, D. W.; Sharp, P. R. *Inorg. Chem.* **1993**, *32*, 612−620.
(40) Srivastava, R. S.; Khan, M. A.; Nicholas, K. M. *J. Am. Chem. Soc.* **2005**, *127*, 7278−7279.
(41) Liebeskind, L. S.; Sharpless, K. B.; Wilson, R. D.; Ibers, J. A. *J. Am. Chem. Soc.* **1978**, *100*, 7061−7063.
(42) Packett, D. L.; Trogler, W. C.; Rheingold, A. L. *Inorg. Chem.* **1987**, *26*, 4308−4309.
(43) Skoog, S. J.; Campbell, J. P.; Gladfelter, W. L. *Organometallics* **1994**, *13*, 4137−4139.
(44) Berman, R. S.; Kochi, J. K. *Inorg. Chem.* **1980**, *19*, 248−254.
(45) Rehorek, D. *Chem. Soc. Rev.* **1991**, *20*, 341−353.
(46) *Electron Paramagnetic Resonance: A Practitioner's Toolkit;* Brustolon, M., Giamello, E., Eds.; John Wiley and Sons, Inc.: Hoboken, NJ, 2009.
(47) Swanwick, M. G.; Waters, W. A. *J. Chem. Soc. B* **1971**, 1059−1064.
(48) Hudson, A.; Lappert, M. F.; Lednor, P. W.; Nicholson, B. K. *J. Chem. Soc., Chem. Commun.* **1974**, 966−967.
(49) Labios, L. A.; Millard, M. D.; Rheingold, A. L.; Figueroa, J. S. *J. Am. Chem. Soc.* **2009**, *131*, 11318−11319.
(50) Iwasa, T.; Shimada, H.; Takami, A.; Matsuzaka, H.; Ishii, Y.; Hidai, M. *Inorg. Chem.* **1999**, *38*, 2851−2859.
(51) Chan, S.-C.; England, J.; Lee, W.-C.; Wieghardt, K.; Wong, C.-Y. *ChemPlusChem* **2013**, *78*, 214−217.
(52) Tomson, N. C.; Labios, L. A.; Weyhermüller, T.; Figueroa, J. S.; Wieghardt, K. *Inorg. Chem.* **2011**, *50*, 5763−5776.
(53) Fox, B. J.; Sun, Q. Y.; DiPasquale, A. G.; Fox, A. R.; Rheingold, A. L.; Figueroa, J. S. *Inorg. Chem.* **2008**, *47*, 9010−9020.
(54) Fox, B. J.; Millard, M. D.; DiPasquale, A. G.; Rheingold, A. L.; Figueroa, J. S. *Angew. Chem., Int. Ed.* **2009**, *48*, 3473−3477.
(55) Ditri, T. B.; Fox, B. J.; Moore, C. E.; Rheingold, A. L.; Figueroa, J. S. *Inorg. Chem.* **2009**, *48*, 8362−8375.
(56) Stewart, M. A.; Moore, C. E.; Ditri, T. B.; Labios, L. A.; Rheingold, A. L.; Figueroa, J. S. *Chem. Commun.* **2010**, *47*, 406−408.
(57) Margulieux, G. W.; Weidemann, N.; Lacy, D. C.; Moore, C. E.; Rheingold, A. L.; Figueroa, J. S. *J. Am. Chem. Soc.* **2010**, *132*, 5033−5035.
(58) Carpenter, A. E.; Margulieux, G. W.; Millard, M. D.; Moore, C. E.; Weidemann, N.; Rheingold, A. L.; Figueroa, J. S. *Angew. Chem., Int. Ed.* **2012**, *51*, 9412−9416.
(59) Barnett, B. R.; Moore, C. E.; Rheingold, A. L.; Figueroa, J. S. *J. Am. Chem. Soc.* **2014**, *136*, 10262−10265.
(60) Carpenter, A. E.; Mokhtarzadeh, C. C.; Ripatti, D. S.; Havrylyuk, I.; Kamezawa, R.; Moore, C. E.; Rheingold, A. L.; Figueroa, J. S. *Inorg. Chem.* **2015**, *54*, 2936−2944.
(61) Wieghardt, K. *Adv. Inorg. Bioinorg. Mech.* **1984**, *3*, 213−274.
(62) *NMR of Paramagnetic Molecules;* La Mar, G. N., Horrocks, W. D., Holm, R. H., Eds.; Academic Press: New York, NY, 1973.
(63) Bowman, A. C.; Milsmann, C.; Atienza, C. C. H.; Lobkovsky, E.; Wieghardt, K.; Chirik, P. J. *J. Am. Chem. Soc.* **2010**, *132*, 1676−1684.
(64) Pizzotti, M.; Porta, F.; Cenini, S.; Demartin, F.; Masciocchi, N. *J. Organomet. Chem.* **1987**, *330*, 265−278.
(65) Brouwer, E. B.; Legzdins, P.; Rettig, S. J.; Ross, K. J. *Organometallics* **1994**, *13*, 2088−2091.
(66) Ridouane, F.; Sanchez, J.; Arzoumanian, H.; Pierrot, M. *Acta Crystallogr., Sect. C* **1990**, *46*, 1407−1410.
(67) Dutta, S. K.; McConville, D. B.; Youngs, W. J.; Chaudhury, M. *Inorg. Chem.* **1997**, *36*, 2517−2522.
(68) Graham, P. M.; Buschhaus, M. S. A.; Baillie, R. A.; Semproni, S. P.; Legzdins, P. *Organometallics* **2010**, *29*, 5068−5072.

DOI: 10.1021/acs.inorgchem.5b01252
Inorg. Chem. 2015, 54, 7110−7121

(69) Carpenter, A. E.; Wen, I.; Moore, C. E.; Rheingold, A. L.; Figueroa, J. S. *Chem.—Eur. J.* **2013**, *19*, 10452−10457.
(70) In the absence of added equivalents of nitrosobenzene, the isocyanate $OCNAr^{Dipp2}$ (**3**) and azoxybenzene are slowly produced from equilibrated mixtures of $Pd(\kappa^1\text{-}N\text{-}PhNO)_2(CNAr^{Dipp2})_2$ (**1a**) and $Pd(\eta^2\text{-}N,O\text{-}PhNO)(CNAr^{Dipp2})_2$ (**2a**), presumably via reaction between **2a** and liberated PhNO. However, formation of **3** and azoxybenzene is greatly accelerated upon addition of excess PhNO.
(71) Otsuka, S.; Aotani, Y.; Tatsuno, Y.; Yoshida, T. *Inorg. Chem.* **1976**, *15*, 656−660.
(72) Cenini, S.; Porta, F.; Pizzotti, M.; La Girolamo, M. *J. Chem. Soc., Dalton Trans.* **1984**, 355−358.
(73) Jones, C. J.; McCleverty, J. A.; Rothin, A. S. *J. Chem. Soc., Dalton Trans.* **1985**, 401−403.
(74) Wiese, S.; Kapoor, P.; Williams, K. D.; Warren, T. H. *J. Am. Chem. Soc.* **2009**, *131*, 18105−18111.
(75) For an example of the trapping of a mono-coordinated Pd(0)-L fragment, see: Fantasia, S.; Nolan, S. P. *Chem.—Eur. J.* **2008**, *14*, 6987−6993.
(76) Lutz, R. E.; Lytton, M. R. *J. Org. Chem.* **1937**, *2*, 68−75.
(77) Colón, D.; Weber, E. J.; Anderson, J. L.; Winget, P.; Suárez, L. A. *Environ. Sci. Technol.* **2006**, *40*, 4449−4454.
(78) Single crystals of $Pd(\kappa^1\text{-}N\text{-}m\text{-}CH_3\text{-}C_6H_4NO)_2(CNAr^{Dipp2})_2$ (**1d**) were analyzed by X-ray diffraction, but the data possessed severe whole molecule positional disorder that could not be satisfactorily modeled. While the crystallographic data were consistent with a mutually trans orientation of the two nitroxide ligands, precise N−O bond lengths could not be determined. Solid-state IR and combustion analysis data are included in the Supporting Information.
(79) Repeated attempts to grow single crystals suitable for X-ray diffraction of the *p*-Br or *p*-Ph substituted metalloxaziridines **2f** or **2i** were unsuccessful.
(80) As freshly prepared solutions of the bis-nitroxide diradicals **1k** or **1l** do contain small amounts of the corresponding metalloxaziridines **2k** or **2l**, precise magnetic moment determinations by Evans method are not possible. However, we do note that the values observed (ca. 1.9 μ_B) are close to those observed in the solid state at ca. 290 K for **1k-l** by SQUID magnetometry (see Figure 11).
(81) Hansch, C.; Leo, A.; Taft, R. W. *Chem. Rev.* **1991**, *91*, 165−195.
(82) The concept of spin density in an open shell singlet molecule, while a non-physical artifact, is a helpful way to visualize the multireference character of the ground state. These plots are therefore included here for comparison with the physically meaningful spin density representations of paramagnetic molecules. See: Noodleman, L.; Peng, C. Y.; Case, D. A.; Mouesca, J.-M. *Coord. Chem. Rev.* **1995**, *144*, 199−244.

DOI: 10.1021/acs.inorgchem.5b01252
Inorg. Chem. 2015, 54, 7110−7121